



A dihydroindolizino indole derivative selectively stabilizes G-quadruplex DNA and down-regulates c-MYC expression in human cancer cells



Narayana Nagesh^{a,*}, G. Raju^b, R. Srinivas^b, P. Ramesh^c, M. Damoder Reddy^c, Ch. Raji Reddy^c

^a CSIR-Centre for Cellular and Molecular Biology, Uppal Road, Hyderabad 500007, India

^b National Centre for Mass Spectrometry, CSIR-Indian Institute of Chemical Technology, Hyderabad 500007, India

^c Division of Natural Products Chemistry, CSIR-Indian Institute of Chemical Technology, Hyderabad 500007, India

ARTICLE INFO

Article history:

Received 23 July 2014

Received in revised form 3 October 2014

Accepted 7 October 2014

Available online 15 October 2014

Keywords:

Dihydroindolizino indole

ESI-MS

Spectroscopy

Selective stabilization of G-quadruplex DNA

Reduce c-MYC expression

Anticancer activity

ABSTRACT

Background: Telomeric and NHE III1, a c-MYC promoter region is abundant in guanine content and readily form G-quadruplex structures. Small molecules that stabilize G-quadruplex DNA were shown to reduce oncoprotein expression, initiate apoptosis and they may function as anticancer molecules.

Methods: Electrospray ionization mass spectrometry, spectroscopy, isothermal titration calorimetry, Taq DNA polymerase stop assay, real time PCR and luciferase reporter assay. Cell migration assay to find out the effect of derivatives on normal as well as cancer cell proliferation.

Results: Among three different dihydroindolizino indole derivatives, 4-cyanophenyl group attached derivative has shown maximum affinity, selective interaction and higher stability towards G-quadruplex DNA over dsDNA. Further, as a potential G-quadruplex DNA stabilizer, 4-cyanophenyl linked dihydroindolizino indole derivative was found to be more efficient in inhibiting in vitro DNA synthesis, c-MYC expression and cancer cell proliferation among human cancer cells.

Conclusion: The present study reveals that dihydroindolizino indole derivative having 4-cyanophenyl group has potential to stabilize G-quadruplex DNA and exhibit anticancer activity.

General significance: These studies are useful in the identification and synthesis of lead derivatives that will selectively stabilize G-quadruplex DNA and function as anticancer agents.

© 2014 Elsevier B.V. All rights reserved.

1. Introduction

Several small molecules play a crucial role in performing various biological activities. Among the group of biologically active molecules, scaffolds containing nitrogen were classified into separate groups. In that, β -carbolines are considered as an important set of molecules with a higher anticancer activity. They belong to a group of indole alkaloids consisting of the pyridine ring, generally found in plants and animals. They exhibit antitumor activity through DNA intercalation and topoisomerase I and II inhibition [1,2]. Molecules with indole group are widespread in nature and they comprise of various biologically active molecules such as tryptophan, serotonin and several plant based alkaloids. Indole derivatives are well known for their pharmacological properties like anticancer [3,4], antitubercular [5], anti-inflammatory [6–8] and antiasthmatic [9]. Although several anticancer drugs are in clinical use, cancer remains a major threat even today. For all therapeutic purposes, a single molecule cannot function effectively for a long period. Therefore, the design and synthesis of hybrid derivatives have gained prominence [10]. The search for efficient hybrid derivatives to

improve their therapeutic index with lesser side effects remains as a challenge for biologists and chemists even today. These reports prompted us to examine the use of synthetic dihydroindolizino indole derivatives with pyrrole and various pharmacophores attached to dehydrate β -carboline moiety in carrying out several biological activities such as selective interaction and stabilization of G-quadruplex DNA, reduction in the overexpression of oncoprotein and proliferation of tumor cells. Both dihydro β -carboline and pyrrole moieties individually are known to show an anticancer activity. Recently, Ravi Chaniyara et al. synthesized similar hybrid derivatives and reported their improved anticancer activity compared to the individual components [11].

The recent research results involving a non-canonical DNA structures, like G-quadruplex DNA, revealed that they play a crucial role in controlling cancer cell proliferation. Now, it has become a challenging task for researchers to identify suitable derivatives that specifically interact with G-quadruplex DNA and stabilize them. It was shown earlier that molecules that stabilize G-quadruplex DNA has been considered as an attractive target for cancer therapy interventions, namely halting transcription [12,13] and DNA damage response signal [14–16]. A recent literature search reveals that several small molecules that stabilize c-MYC quadruplex DNA will down regulate c-MYC oncogene expression [17–21]. Few recently reported potential molecules that

* Corresponding author. Tel.: +91 4027192568; fax: +91 4027160311.
E-mail address: nagesh@ccmb.res.in (N. Nagesh).

stabilize G-quadruplex DNA complex are, cationic porphyrins [22,23] acridine derivatives [24] ethidium derivatives [25] anthraquinone derivatives [26] perylene derivatives [27] and telomestatin derivatives [28]. Earlier studies from our laboratory, were made to identify suitable derivatives that interact and stabilize the G-quadruplex DNA [29,30].

G-quadruplex DNA was demonstrated to exhibit structural polymorphism under physiological conditions, such as parallel, anti-parallel, and hybrid configurations [31] and helps in performing the targeted biological activity. Their existence has been identified in biologically important regions such as telomeric ends of chromosomes [32], the nuclease hypersensitivity element III1 (NHE III1), a guanine-rich 27 base pair region (Pu27) located upstream of the c-MYC promoter [33], the c-kit promoter region [34], immunoglobulin heavy chain switch region [35] and the trinucleotide repeats present in the FMR1 gene [36]. Although, several researchers have proposed the existence of G-quadruplex structure in cancer cells over the years, only recently, the occurrence of quadruplex was confirmed using a specific antibody that binds to G-quadruplex DNA [37].

Formation of G-quadruplex structures occurs through the stacking of planar G-tetrads held together by Hoogsteen hydrogen bonds that affect biological activities in vitro [38–40]. For the formation of G-quadruplex complex, primarily it requires a monovalent cations such as K^+ , NH_4^+ , and Na^+ in the central cavity [39,40]. G-quadruplexes can fold into various forms in which DNA strands assemble either into intramolecular or intermolecular configurations.

Of late, we have reported the interaction of hybrid β -carboline derivatives with DNA and their biological activity [41]. In continuation, herein we describe the synthesis of hybrid derivatives having dihydro β -carboline and pyrrole groups [dihydroindolizino indoles (DHII)] and studies on their biophysical, biochemical and anticancer properties. The general structure of dihydroindolizino indole derivatives (DHII), the structure of DHII-4CPh, DHII-TPh, and DHII-MPhPy and their general synthesis are presented in Fig. 1.

2. Materials and methods

2.1. Derivative synthesis

To *N*-indoloyl pyrrole (0.5 mM) and aldehyde (0.55 mM) in 4 ml dichloromethane, PTSA (5 mol%) was added at room temperature and continuously stirred for 1 to 4 h. After completion of the reaction, the mixture was diluted with water (5 ml) and extracted with dichloromethane (3×6 ml). The combined organic extracts were washed with brine (10 ml), dried over Na_2SO_4 and concentrated in vacuo. The residue was purified by column chromatography on silica gel (EtOAc: Hexanes) to give the corresponding dihydroindolizino indole derivatives (DHII-4CPh, DHII-TPh and DHII-MPhPy). Characterization of each derivative is shown under supplementary information.

2.2. Preparation of stock solutions of DNA and synthetic hybrid derivatives

In the present study, the G-quadruplex forming DNA sequences from the human telomeric region and nuclear hypersensitivity element III1 (NHE III1) region of the c-MYC promoter were synthesized. The human telomeric region contains several stretches of 5'TTAGGG 3' sequences and the NHE III1 region, placed slightly upstream of the c-MYC promoter is rich in guanine, which was reported earlier to form the G-quadruplex complex [42–44]. Therefore, the oligonucleotides used in the present study such as d(T₂AG₃) and d(T₂AG₃)₂, 27 mer c-MYC quadruplex forming DNA (Pu27), its reverse primer (Pu27 rev) and a mutated sequence of Pu27, that does not form quadruplex DNA structure (Pu27-13, 14) was synthesized using ABI 394 DNA synthesizer (Applied Biosystems, USA) and purified by reverse phase high performance liquid chromatography (RP-HPLC). In order to form the G-quadruplex complex, the d(T₂AG₃) and d(T₂AG₃)₂ oligonucleotide solution was heated to 90 °C and slowly cooled to room temperature. The DNA samples were dialyzed (1000 molecular weight cutoff membrane)

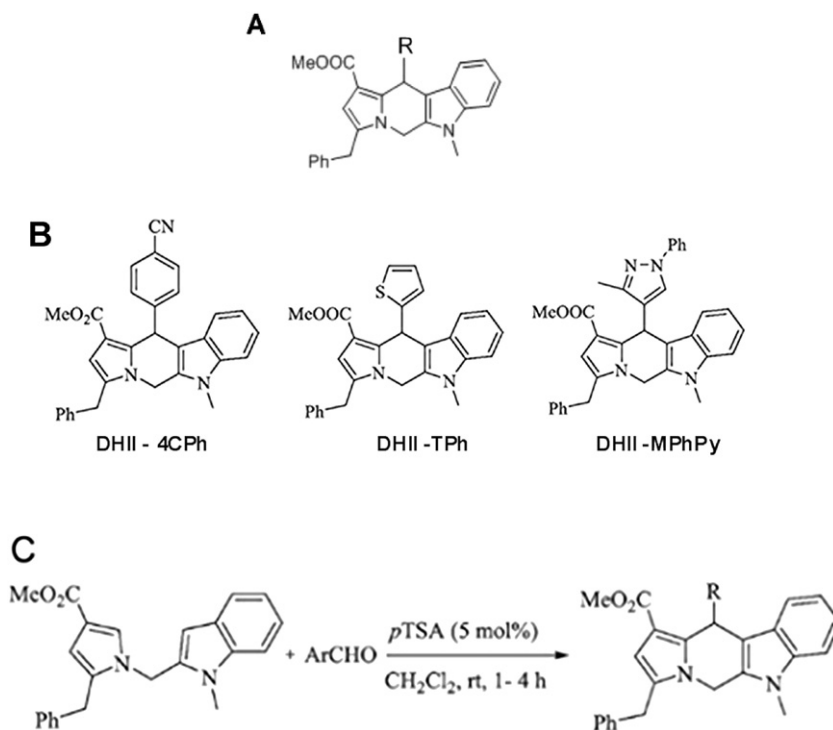


Fig. 1. A. General structure of dihydroindolizino indole derivatives. –R, indicates the placement at which various aryl groups were attached. B. The structures of DHII-4CPh, DHII-TPh and DHII-MPhPy. C. A synthetic scheme for the various dihydroindolizino indole derivatives (DHII-4CPh, DHII-TPh and DHII-MPhPy) used in the present study.

against two changes of 1 l KBPS buffer (30 mM Potassium Phosphate, pH 7.0, with 100 mM KCl, pH 7.0) and incubated at 4 °C for 24 h. The G-quadruplex formed by d(T₂AG₃) and d(T₂AG₃)₂ were used in mass spectrometry and spectroscopy studies, whereas the synthetic DNA from NHE III1 region was utilized for other biochemical assays. Stock solutions of G-quadruplex DNA / synthetic DNA primers (1 mM) were prepared in 100 mM KBPS buffer/TE (pH 7.0). Calf thymus DNA (CT DNA) was purchased from Sigma Aldrich and used without further purification. The stock solution of CT DNA (1 mM) was prepared in TE (pH 7.0). The stock solutions of dihydroindolizino indole derivatives (1 mM) were prepared by dissolving them in 1:1, methanol:water solvent system.

2.3. DNA melting studies

The effect of the synthetic derivatives on DNA stability will be usually studied by monitoring the change in the DNA melting temperature (T_m) in the presence and the absence of each derivative. Melting studies were performed using ABI Lambda Spectrophotometer (Waltham, MA, USA) attached with thermal controller. 25 μM CT DNA and human telomeric G-quadruplex formed by d(T₂AG₃)₂ were taken in 0.1 cm path length quartz cuvette and absorbance was recorded in the absence and the presence of each derivative. CT DNA and G-quadruplex DNA were taken in TE (pH 7.0) and 100 mM KBPS buffer respectively, and 25 μM of each derivative was gradually added and absorbance was recorded at 260 nm. The temperature ramp was maintained at 0.3 °C/s. Each experiment was repeated thrice and the mean value was considered.

2.4. Isothermal titration calorimetry (ITC)

The interaction of each derivative with DNA (both dsDNA and G-quadruplex DNA) was assayed by isothermal titration calorimetry (ITC) using Microcal VP-ITC (Northampton, MA, USA). All the ITC experiments were carried out by filling the ITC cell with 20 mM DNA solution (both d(T₂AG₃)₂ G-quadruplex DNA and CT DNA) and 5 mM of DHII-4CPh, DHII-TPh and DHII-MPhPy derivatives were taken in the titration syringe. Every time, 60 injections (each injection delivers 5 μl) of derivatives were added to ITC cell. The addition of each derivative to G-quadruplex DNA was made at intervals of 180 s. The ITC titration experiment was repeated thrice to eliminate errors generated while performing the experiment. The integrated heat/injection data obtained in each ITC titration were fitted using two independent sites' model to understand the binding affinity of dihydroindolizino indole derivatives to G-quadruplex DNA. It was described earlier [45] that the equilibrium of macromolecules, such as G-quadruplex DNA with multiple ligand binding sites can be exemplified by two different association constants. Thermodynamic parameters such as, ΔG₁, ΔG₂, ΔH₁, ΔH₂, ΔS₁, ΔS₂, K₁ and K₂ were extracted directly from the fits.

2.5. Electrospray ionization mass spectrometry (ESI-MS)

The stoichiometry and binding affinity of the derivative, DHII-4CPh towards dimeric and tetrameric forms of G-quadruplex DNA at a lower concentration (in nanomolar range), mimicking the physiological conditions was studied using ESI-MS on an Exactive Orbitrap mass spectrometer (Thermo Scientific, USA) in negative ion mode. In mass spectral studies, oligonucleotides with lower mass [d(T₂AG₃) and d(T₂AG₃)₂], but nonetheless capable of forming quadruplex structure were used to get clear spectra. Analysis of ESI-MS data can distinguish the dimeric and tetrameric folded forms of G-quadruplex DNA. Data acquisition was made using the Xcalibur software (Thermo Scientific). The source conditions maintained were; sheath gas (N₂) pressure, 35 psi; aux. gas pressure, 5 psi; capillary temperature, 120 °C; capillary voltage, −50.0 V; tube lens offset voltage, −60 V; skimmer voltage, −40 V;

and vaporizer temperature, 50 °C. Scanning parameters were: higher energy collisional induced dissociation (HCD) gas, off; resolution, enhanced; microscans, 1; lock masses, off, AGC target, balanced and maximum injection time, and 200 ms for a full-scan mass spectrum. For ESI-MS experiments, the concentration of intermolecular G-quadruplex DNA (both d(T₂AG₃) and d(T₂AG₃)₂) and derivative was maintained at 10 nM. All the sample solution was infused into the ESI source at a flow rate of 5 μl/min by using the instrument's syringe pump and the spectra were recorded under identical experimental conditions for all compounds with an average of 25–30 scans.

2.6. Circular dichroism (CD) spectroscopy

DNA conformational studies were carried out on a JASCO 815 CD spectropolarimeter (Jasco, Tokyo, Japan). Spectroscopic studies were performed to study the interaction of DHII-4CPh with G-quadruplex DNA [both d(T₂AG₃) and d(T₂AG₃)₂] at a micro molar concentration range. G-quadruplex DNA solution was prepared in 100 mM KBPS buffer. To 5.0 μM of G-quadruplex DNA formed by d(T₂AG₃) and d(T₂AG₃)₂, 2.5 μM and 5.0 μM DHII-4CPh was added and CD spectra was recorded from 220 nm to 320 nm with a 1 mm path length cuvette. The spectra were averaged over 3 scans.

2.7. UV-visible spectroscopy

UV-visible absorption spectra were recorded using ABI 35 Lambda Spectrophotometer (Waltham, MA, USA) at 25 °C. All the experiments were carried out in polystyrene cuvettes to minimize binding of derivatives to the surface of the cuvettes. 5.0 μM of DHII-4CPh and 5.0 μM G-quadruplex DNA was prepared in 1:1, methanol:milliQ water and 100 mM KBPS buffer respectively. About 1 ml of 5.0 μM DHII-4CPh was taken in a 1 cm path length cuvette and each time 5 μl of G-quadruplex DNA formed by d(T₂AG₃) and d(T₂AG₃)₂ was added. Absorption spectra were recorded in the range of 200 nm to 350 nm. All the solutions were freshly prepared before commencing the experiment and titration was carried out until saturation of absorbance occurs.

Absorbance values were recorded after each successive addition of DNA solution and equilibrated for about 5 min. The data obtained was fitted in Eq. (1), to obtain binding constant, K_b.

$$\frac{[\text{DNA}]}{(\epsilon_a - \epsilon_f)} = \frac{[\text{DNA}]}{(\epsilon_b - \epsilon_f)} + \frac{1}{K_b(\epsilon_b - \epsilon_f)} \quad (1)$$

where ϵ_a , ϵ_f and ϵ_b are the apparent, free and bound complex extinction coefficients, respectively. In particular, ϵ_f was found from the calibration curve of the isolated DHII-4CPh in solution and by following the Beer's law ϵ_a was determined as the ratio between the measured absorbance and DHII-4CPh concentration, Absorbance / [DHII-4CPh]. A plot of [DNA] / ($\epsilon_a - \epsilon_f$) vs. [DNA] provide the slope of 1 / ($\epsilon_b - \epsilon_f$) and the intercept Y is equal to 1 / K_b ($\epsilon_b - \epsilon_f$). The ratio of the slope to the Y intercept provides the binding constant (K_b).

2.8. PCR stop assay

In this assay, the effect of dihydroindolizino indole derivatives (DHII) on c-MYC G-quadruplex DNA stabilization followed by inhibition of in vitro DNA synthesis was studied. This assay was carried out by adopting the protocol described earlier [46]. The nuclear hypersensitivity element III1 (NHE III1) region, present upstream of c-MYC P1 promoter, that controls 80–90% of c-MYC transcription, was taken as a template in the PCR stop assay. The 27 base DNA strand (Pu27) and its complementary strand (Pu27 Rev) were employed in this assay. Further, a mutated Pu27 strand, in which the guanines at the 13th and 14th positions were changed to adenosines (Pu27-13, 14) was

considered to examine the effect of the derivatives on non-G-quadruplex forming DNA. The positions indicating base modifications in Pu27-13, 14 are shown in bold. The DNA sequences used in the PCR stop assay are shown in the following table.

S. no	Name of the oligonucleotide	Sequence of a DNA strand
1.	Pu27	5'-TGGGGAGGGTGGGGAGGGTGGGAAGG-3'
2.	Pu27 rev	5'-ATCGATCGC TTCTCGTCTCCCA-3'
3.	Pu27-13,14	5'-TGGGGAGGGTGG AA GGGTGGGAAGG-3'

To the PCR mixture (25 μ l) containing 10 mM Tris-HCl (pH 8.3), with 50 mM KCl, 1.5 mM Mg(OAc)₂, 5 μ M of Pu27 and Pu27 rev oligonucleotides incubated at 4 °C for 6 h with various concentrations (2 μ M, 4 μ M, 6 μ M, and 8 μ M) of DHII-4CPh, DHII-TPh and DHII-MPhPy, 1 mM dNTPs, 5 units of *Taq* DNA polymerase were added and PCR reactions were performed. PCR reaction was also carried out under the same conditions with Pu27-13, 14 and Pu 27 rev, in the presence of 2 μ M to 8 μ M concentration of DHII-4CPh alone, because it showed maximum inhibition with Pu27 quadruplex. PCR carried out with 27 base DNA strand (Pu27) and its complementary strand (Pu27 Rev) in the absence of the dihydroindolizino indole derivative was considered as control. Stop assay with control, Pu27 and the mutant form of Pu27 namely Pu2-13, 14 samples will not only argue the role of each derivative on G-quadruplex stabilization followed by inhibition of in vitro DNA synthesis but also it will help to evaluate the derivative's effect on the inhibition of polymerase. Stop assay was performed using the ABI thermal cycler (Foster City, CA, USA). Initial denaturation was performed at 94 °C for 3 min, followed by 20 repeated cycles each having 94 °C for 30 s, 58 °C for 30 s, and 72 °C for 30 s. After PCR, 5 μ l of the amplified product was loaded on a 12% non-denaturing polyacrylamide gel with 1 \times TBE. The in vitro DNA synthesis band intensity was measured using Bio Rad Gel Doc XR+ system (USA). Percentage inhibition of DNA synthesis was calculated using Eq. (2) and the inhibition constant K_i for each dihydroindolizino indole derivative was calculated by using Eq. (3) (Cheng–Prusoff equation).

$$\text{Percentage of inhibition} = \frac{C-L}{C} \times 100 \quad (2)$$

C — band intensity with control.

L — band intensity with derivative.

$$\text{Inhibition constant } (K_i) = 1 + \frac{IC_{50}}{K_m [dNTP]} \quad (3)$$

IC_{50} — half maximal inhibitory concentration.

[dNTP] — concentration of dNTPs used.

K_m — Michaelis constant.

2.9. Luciferase reporter assay

Role of G-quadruplex DNA stabilization by a synthetic dihydroindolizino indole derivatives and subsequent inhibition of gene expression was evaluated using the luciferase reporter assay. About 1×10^6 HeLa cells were seeded and grown in DMEM medium supplemented with 10% FCS in a six-well plate. The Del 4 plasmid (a

gift from Vogelstein laboratory) which harbors the 22-mer c-MYC quadruplex forming sequence was cloned slightly upstream of the luciferase reporter gene. Likewise, in Del 4 mutant plasmid (a gift from Chowdhury laboratory) instead of c-MYC, a mutated DNA sequence, which does not form a G-quadruplex structure [47] due to G to A change was cloned. In Del 4 mutant plasmid also, the mutated DNA sequence was cloned slightly upstream of the luciferase reporter gene. The DNA sequences used in the Del 4 and Del 4 mutant plasmids are shown below.

S. no.	Name of the plasmid	DNA sequences cloned
1.	Del 4	5'-GGGGAGGGTGGGGAGGGTGGGG-3'
2.	Del 4 mutant	5'-GGGGAGGGTGAAGAGAGTGGGG-3'

About 1 μ g of Del-4 or Del-4 mutant plasmid was transfected into HeLa cells grown to 75% confluency using Lipofectamine 2000 as per manufacturer's protocol. After 5 h of transfection, the cells were washed twice with PBS and fresh media was added. The cells were treated with 0 μ M, 2 μ M, 4 μ M, 6 μ M and 8 μ M of DHII-4CPh for 24 h and 48 h. The cells were then lysed with Cell Culture Lysis Reagent (CCLR) buffer (Promega Luciferase Assay System Cat No-E1500) with continuous pipetting at 48 °C for 30 min. Luciferase expression was determined using a Dual Luciferase assay kit (Promega) on chemi-luminescence detection system (Chemi-Smart 5000, Vilber Lourmat, Germany). The samples in the presence of DHII-4CPh were normalized with the data obtained in the absence of derivatives. All the experiments were repeated thrice to minimize errors.

2.10. Real time PCR for gene expression

Exponentially growing B16F10 melanoma cancer cells (1×10^6) in Dulbecco's Modified Eagle Medium (DMEM), supplemented with 10% Fetal Calf Serum (FCS) were seeded in six well plates. The B16F10 cells were processed with different concentrations of DHII-4CPh, (0 μ M, 2 μ M, 4 μ M, 6 μ M and 8 μ M) for 24 h. The cells to which no dihydroindolizino indole derivative added was considered as control and they were incubated for 24 h under similar conditions. After 24 h of treatment, the cells were lysed using Trizol reagent (Invitrogen) [48] and RNA was extracted. To about 1 μ g of total RNA, 20 μ l reaction mixture containing 1 \times Moloney Murine Leukemia Virus Reverse Transcriptase buffer (M-MLV buffer) from Promega (catalogue no. M5313), 500 μ M dNTP, 100 pmol oligo dT primer, and 100 units of M-MLV reverse transcriptase (from Promega), DEPC-H₂O was added. Mixtures were incubated at 42 °C for 60 min for reverse transcription and then at 92 °C for 10 min to inactivate the enzyme. PCR was performed by preparing 20 μ l reaction mixture contained 1 \times PCR buffer, 500 μ M dNTPs, 0.15 μ M β -actin primers, 1.5 μ M c-MYC primers, 1 unit of *Taq* polymerase, 0.1% DEPC-H₂O, and 3 μ l of the cDNA template. The PCR reaction was carried out in an ABI Perkin Elmer Thermal Cycler and the product was amplified. The amplification conditions are as follows: 95 °C for 5 min, followed by 36 cycles of 95 °C for 1 min, 50 °C for 1 min, and 72 °C for 1 min. The amplified products were separated on a 1.5% agarose gel, and photographs were taken on a Bio-Rad Gel Doc XR+ system (USA). Expression of β -Actin was used as a reference in the real time PCR experiment. The c-MYC and β -actin primers used in real time PCR are given below.

S. no.	Name of the primer	DNA sequence
1.	c-MYC-F	5' TGAGGAGACACCGCCAC 3'
2.	c-MYC-R	5' CAACATCGATTCTTCCTCATCTTC 3'
3.	β -Actin-F	5' AAGAGAGGCATCTCACCT 3'
4.	β -Actin-R	5'TACATGGCTGGGGTGTGAA 3'

2.11. Cell migration assay

Normal and cancer cells were seeded at 20,000–40,000 cells/cm² with 0.2 ml/cm² media and incubated for 48 h at 37 °C, 6% CO₂, 95% relative humidity. The DHII-4CPh, DHII-TPh and DHII-MPhPy derivatives were added to the cells at different concentrations (0 μM, 2 μM, 4 μM, 6 μM, 8 μM, 10 μM, 15 μM, 25 μM, 50 μM) and the cells were incubated for 24 h. Cells treated with Hermine in the same concentration range was considered as control. Cancer cells were seeded into a six-well tissue culture dish and allowed to grow to 90% confluence in a complete medium. Sufficient care was taken to grow the cells in a single monolayer. A sterilized plastic tip (1 mm) that touched the plate as described [49] wounded cell monolayers. Wounded monolayers were then washed four times with medium to remove cell debris and incubated in 0.5% FBS medium in the absence or in the presence of dihydroindolizino indole derivatives (DHII) and admitted it to grow for 24 h. Cells were monitored under a microscope fitted with a camera (Zeiss).

2.12. Statistical analysis

The data procured from different experiments were subjected to statistical analysis using Student's two-tailed unpaired *t*-test using Graphpad Prism software version 4.0 (San Diego, CA, USA). Data was considered significant if *p* value ≤ 0.05.

3. Results and discussion

3.1. Synthesis of dihydroindolizino indole derivatives

The dihydroindolizino indole derivatives (DHII) were synthesized from the reaction of *N*-indolyl pyrrole with aromatic aldehydes in the presence of pTSA (5 mol%) in dichloro-methane at room temperature [50]. Initially, 4-cyano benzaldehyde was used as an aldehyde component, which provided the dihydroindolizino indole derivative with 4-cyanophenyl group (DHII-4CPh) in 86% yield. Likewise, various aromatic aldehydes having different substitutions and heteroaromatic aldehydes successfully provided the corresponding dihydroindolizino indole derivatives (DHII-4CPh, DHII-TPh and DHII-MPhPy) in good yield. The dihydroindolizino indole derivatives primarily consist of dihydro β-carboline, pyrrole and various aryl substituents to produce different aryl-substituted dihydroindolizino indole derivatives (DHII-4CPh, DHII-TPh and DHII-MPhPy). The β-carboline and β-carboline-like structures (depicted in dark black color) in dihydroindolizino indole and the position of aryl groups in dihydroindolizino indole are shown in Fig. S1 (under supplementary information).

3.2. Interaction and stabilization of G-quadruplex DNA by dihydroindolizino indole derivatives

3.2.1. G-quadruplex DNA and dsDNA melting in the presence of synthetic indole derivatives

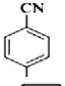
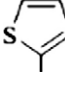
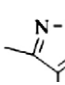
DNA melting studies are useful to identify the potential of derivatives in stabilizing DNA. In order to understand the extent of stability provided to different forms of DNA by synthetic DHII derivatives, melting studies were carried out in the presence of G-quadruplex DNA formed by d(T₂AG₃)₂ and CT DNA. The increase in Δ*T*_m of the DNA-derivative complex is consistent with higher stabilization of the complex by the interacting derivative. The melting temperatures (*T*_m) of CT DNA and G-quadruplex DNA formed by d(T₂AG₃)₂ alone were found to be 69.8 °C and 54.8 °C respectively. The difference in melting temperature (Δ*T*_m) of CT DNA and G-quadruplex DNA in the presence of each derivative is shown in Table 1. In general, with all the derivatives, Δ*T*_m with G-quadruplex DNA was higher than CT DNA, indicating their ability to stabilize G-quadruplex DNA better than dsDNA. Among the dihydroindolizino indole (DHII) derivatives studied, DHII-4CPh exhibited maximum variation in Δ*T*_m with both kinds of DNA. The Δ*T*_m of DHII-4CPh–quadruplex DNA complex was found maximum (Δ*T*_m ≈ 17 °C), suggesting that the dihydroindolizino indole derivatives with 4-cyanophenyl group as a pharmacophore (DHII-4CPh) interact and stabilize G-quadruplex DNA much better than other derivatives selected in the present study [51,52].

3.2.2. Higher affinity and interaction of DHII-4CPh with G-quadruplex DNA compared to dsDNA

Isothermal titration calorimetry (ITC) is a sensitive microcalorimetric technique for determining derivative's binding affinity, stoichiometry and thermodynamic parameters of DNA-derivative complex [53]. To corroborate the DNA melting data and to find the role of DHII-4CPh in selective interaction and stabilization of G-quadruplex DNA, ITC titrations were carried out with DHII-4CPh, DHII-TPh and DHII-MPhPy derivatives using both forms of DNA (G-quadruplex and CT DNA). ITC thermograms of DHII-4CPh, DHII-TPh and DHII-MPhPy after interaction with d(T₂AG₃)₂ G-quadruplex are shown in Fig. 2. It is obvious from the ITC results that derivative's binding to quadruplex DNA occurs in two ways, one with higher and another with lower affinity. The first one takes place with the considerable entropy change (−3.0 to −8.0 kcal/mol) and the second process proceeds with a significant change in enthalpy (−6.0 to −8.0 kcal/mol). Although the variation in entropy and enthalpy alone is not sufficient to determine the molecular interaction with DNA. However, the significant thermodynamic changes observed due to interaction between the derivative and the DNA bases will provide a much closer view of their interaction [54]. The binding constants of derivatives in the foremost and second mode are in the order of 10^{−7} and 10^{−5} respectively. Further, the binding

Table 1

The Δ*T*_m values obtained with different DNA-DHII derivatives. The melting temperatures of CT DNA and G-quadruplex DNA formed by d(T₂AG₃)₂ in the absence of any derivative is 69.8 °C and 54.8 °C respectively.

s. no	Derivative name	–R	Δ <i>T</i> _m (°C) Duplx DNA	Δ <i>T</i> _m (°C) G-quadruplex DNA
1.	DHII-4CPh		5.6 ± 0.3	16.7 ± 0.7
2.	DHII-TPh		4.1 ± 0.5	10.7 ± 0.9
3.	DHII-MPhPy		4.5 ± 0.7	10.3 ± 0.7

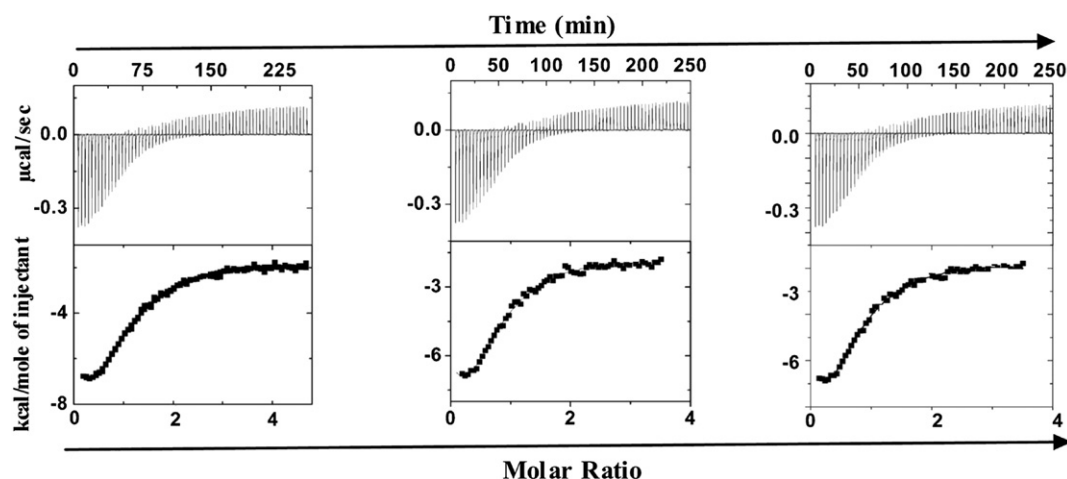


Fig. 2. ITC thermogram obtained on titration between $d(T_2AG_3)_2$ G-quadruplex DNA and DHII-4CPh, DHII-TPh and DHII-MPhPy.

constants (K_1 and K_2) with DHII-4CPh are comparatively high, showing good interaction of DHII-4CPh with $d(T_2AG_3)_2$ G-quadruplex DNA. ITC results, shown in Table 2, support the data obtained from DNA melting experiments. From the ITC thermogram, it is evident that the stoichiometry between $d(T_2AG_3)_2$ G-quadruplex: DHII-4CPh is 1:2.

Further, saturation of the ITC signal in the titration between DHII-4CPh and CT DNA (dsDNA), occurs in less time (about 30 min) when compared to G-quadruplex DNA (about 250 min), emphasizes lesser interaction of DHII-4CPh with CT DNA compared to intermolecular G-quadruplex DNA formed by $d(T_2AG_3)_2$. The ITC thermogram obtained on addition of DHII-4CPh to CT DNA is shown in Fig. S2 (under supplementary information). ITC data also substantiate that among the potential derivatives, DHII-4CPh showed maximum interaction with G-quadruplex DNA than with CT DNA (dsDNA).

3.3. Interaction and binding between 4-cyanophenyl dihydroindolizino indole derivatives (DHII-4CPh) and G-quadruplex DNA

3.3.1. ESI-MS studies to understand the interaction of DHII-4CPh with two different forms of intermolecular G-quadruplex DNA

From the DNA melting and ITC experiments, it is evident that DHII-4CPh has better interaction with G-quadruplex DNA compared to dsDNA. It is hard to conclude from the above experimental results, which form of G-quadruplex DNA has a higher interaction with DHII-4CPh. ESI-MS studies were performed to find the difference in the interaction and the binding stoichiometry of DHII-4CPh toward two forms of intermolecular human G-quadruplex DNA (dimeric and tetrameric) at a lower concentration (in the nM range). ESI-MS is a soft ionization technique, which allows detection of intact non-covalent complexes, especially at a low concentration [55,56]. Ammonium acetate was used as

buffer to obtain clean spectra and 10% methanol to improve spraying conditions [57]. To look into the interaction of DHII-4CPh with both the G-quadruplex sequences, negative ion ESI mass spectra were recorded and the details are given in Table 3. The mass spectrum of G-rich single strand $d(5'TTAGGG3')$ or $d(T_2AG_3)$ exhibits deprotonated ions at m/z 614, 922, 933, 942, and 947 (Fig. 3A). The ions at m/z 614 ($[SS]^{3-}$) and m/z 922 ($[SS]^{2-}$) are imputed to the single stranded structure of $d(T_2AG_3)$ with the charge states of -3 and -2 respectively. The peaks at m/z 933 ($[Q_a + 2 K-H]^{8-}$), m/z 942 ($[Q_a + 4 K-H]^{8-}$), and m/z 947 ($[Q_a + 5 K-H]^{8-}$) correspond to the intermolecular G-quadruplex DNA formed by tetrameric $d(T_2AG_3)$ structure with the charge states of -8 , -8 , and -8 respectively. ESI-MS data indicate that $d(T_2AG_3)$ oligonucleotide can form only tetrameric G-quadruplex.

We speculate that five cations stabilize the G-quadruplex DNA formed by $d(T_2AG_3)$. Of these, three ions are connected to guanines and other two cations are associated with thymidines. It was shown earlier that besides guanines, thymidines also form clusters stabilized by cations [58]. Since cations were shown to lodge in the cavity in the center of quadruplex [59] the ammonium and potassium cations were placed in the pith of the G-quadruplex formed by $d(T_2AG_3)$.

Fig. 3B displays the negative ion ESI mass spectrum obtained when $d(T_2AG_3)$ G-quadruplex interacts with DHII-4CPh. The spectrum exhibits the peaks at m/z 530 ($[Q_a + \text{DHII-4CPh} + 3 K-H]^{15-}$), m/z 614 ($[SS]^{3-}$), m/z 922 ($[SS]^{2-}$), m/z 933 ($[Q_a + 2 K-H]^{8-}$), m/z 942 ($[Q_a + 4 K-H]^{8-}$), m/z 947 ($[Q_a + 5 K-H]^{8-}$) and m/z 1003 ($[Q_a + \text{DHII-4CPh} + 4 K + \text{NH}_4-3H]^{8-}$). The ions at m/z 530 ($[Q_a + \text{DHII-4CPh} + 3 K-H]^{15-}$) and m/z 1003 ($[Q_a + \text{DHII-4CPh} + 4 K + \text{NH}_4-3H]^{8-}$) can be attributed to the adduct ions formed by the interaction between DHII-4CPh and G-quadruplex DNA with the charge states of -15 and -8 respectively. It is interesting to note that DHII-4CPh interact with a tetrameric form of $d(T_2AG_3)$ G-quadruplex DNA at 1:1 stoichiometry. Further, it is apparent that less number of DHII-4CPh- $d(T_2AG_3)$ G-quadruplex DNA complex adduct peaks were observed in the ESI-MS spectra (Fig. 3B) indicating comparatively lower interaction of DHII-4CPh with the tetrameric form of G-quadruplex formed by $d(T_2AG_3)$.

The negative ion ESI mass spectrum of G-rich single strand $d(5'TTAGGGTTAGGG3')$ or $d(T_2AG_3)_2$ shows the deprotonated ions at m/z 770 ($[Q_b + 5 K-H]^{10-}$), m/z 938 ($[SS]^{4-}$), m/z 952 ($[Q_b + 3 K-H]^{8-}$), m/z 1251 ($[SS]^{3-}$), m/z 1270 ($[Q_b + 3 K-H]^{6-}$), and m/z 1508 ($[Q_b + 2\text{NH}_4-H]^{5-}$) (Fig. 3C). The ions at m/z 938 ($[SS]^{4-}$) and m/z 1251 ($[SS]^{3-}$) can be attributed to the single-stranded structure of $d(T_2AG_3)_2$ sequence with the charge states of -4 and -3 , respectively. Peaks at m/z 770 ($[Q_b + 5 K-H]^{10-}$), m/z 952 ($[Q_b + 3 K-H]^{8-}$), m/z 1270 ($[Q_b + 3 K-H]^{6-}$), and m/z 1508 ($[Q_b + 2\text{NH}_4-H]^{5-}$) correspond to the dimeric structures (G-quadruplex having two hairpin DNA

Table 2

ITC data obtained when DHII-4CPh, DHII-TPh and DHII-MPhPy interact with $d(T_2AG_3)_2$ G-quadruplex DNA complex..

ITC derived thermodynamic parameters	DHII-4CPh-quadruplex DNA	DHII-TPh-quadruplex DNA	DHII-MPhPy-quadruplex DNA
$K_1 \times 10^{-7}$	4.27 (± 0.4)	1.65 (± 0.09)	1.12 (± 0.03)
ΔG_1 (kcal/mol)	-10.45	-9.78	-8.37
ΔH_1 (kcal/mol)	-2.42 (± 0.1)	-4.27 (± 0.07)	-4.96 (± 0.05)
ΔS_1 (kcal/mol)	-8.03	-5.51	-3.41
$K_2 \times 10^{-5}$	5.26 (± 0.6)	2.61 (± 0.3)	2.14 (± 0.2)
ΔG_2 (kcal/mol)	-7.70	-7.88	-8.91
ΔH_2 (kcal/mol)	-5.79 (± 0.1)	-6.86 (± 0.08)	-7.54 (± 0.09)
ΔS_2 (kcal/mol)	-1.91	-1.02	-1.37

Table 3ESI-MS data obtained when DHII-4CPh derivative interact with d(T₂AG₃) and d(T₂AG₃)₂ G-quadruplex DNA.

G-quadruplex	Derivative	m/z (relative abundance)	Charge of the complex	Quadruplex: derivative
d(T ₂ AG ₃)	No derivative	614 (12)	([SS] ^{3−})	0:0
		922 (100)	([SS] ^{2−})	0:0
		933 (10)	[Q _a + 2 K-H] ^{8−}	1:0
		942 (06)	[Q _a + 4 K-H] ^{8−}	1:0
		947 (22)	[Q _a + 5 K-H] ^{8−}	1:0
d(T ₂ AG ₃)	DHII-4CPh	530 (100)	[Q _a + DHII-4CPh + 3 K-H] ^{15−}	1:1
		614 (19)	([SS] ^{3−})	0:0
		922 (66)	([SS] ^{2−})	0:0
		933 (06)	[Q _a + 2 K-H] ^{8−}	1:0
		942 (03)	[Q _a + 4 K-H] ^{8−}	1:0
		947 (28)	[Q _a + 5 K-H] ^{8−}	1:0
		1003 (06)	[Q _a + DHII-4CPh + 4 K + NH ₄ -3H] ^{8−}	1:1
		770 (28)	[Q _b + 5 K-H] ^{10−}	1:0
		938 (50)	[SS] ^{4−}	0:0
		952 (20)	[Q _b + 3 K-H] ^{8−}	1:0
d(T ₂ AG ₃) ₂	No derivative	1251 (100)	[SS] ^{3−}	0:0
		1270 (31)	[Q _b + 3 K-H] ^{6−}	1:0
		1508 (10)	[Q _b + 2NH ₄ -H] ^{5−}	1:0
		696 (30)	[Q _b + 4 K-H] ^{11−}	1:0
		770 (30)	[Q _b + 5 K-H] ^{10−}	1:0
		977 (15)	[Q _b + DHII-4CPh + 4 K-H] ^{16−}	1:1
		1001 (100)	[Q _b + DHII-4CPh + K-H] ^{8−}	1:1
		1017 (13)	[Q _b + DHII-4CPh + 4 K-H] ^{8−}	1:1
		1074 (06)	[Q _b + 2DHII-4CPh + 3 K + NH ₄ -H] ^{8−}	1:2
		1257 (08)	[Q _b + K-H] ^{6−}	1:0
d(T ₂ AG ₃) ₂	DHII-4CPh	1508 (10)	[Q _b + 2NH ₄ -H] ^{5−}	1:0

Q_a = G-quadruplex DNA formed by four strands (tetrameric form) of d(T₂AG₃) and Q_b = G-quadruplex DNA formed by two hairpin strands (dimeric form) of d(T₂AG₃)₂.

strands) formed by d(T₂AG₃)₂ with the charge states of −10, −8, −6, and −5, respectively (Table 3). The m/z values in the ESI-MS spectra, exactly correspond with two strands of d(T₂AG₃)₂ instead of four strands of d(T₂AG₃)₂ indicating the presence of the dimeric form of G-quadruplex DNA in solution.

Fig. 3D shows the ESI-MS spectrum of d(T₂AG₃)₂G-quadruplex after interaction with DHII-4CPh. The spectrum exhibits the ions at m/z 696 ([Q_b + 4 K-H]^{11−}), m/z 770 ([Q_b + 5 K-H]^{10−}), m/z 977 ([Q_b + DHII-4CPh + 4 K-H]^{16−}), m/z 1001 ([Q_b + DHII-4CPh + K-H]^{8−}), m/z 1017 ([Q_b + DHII-4CPh + 4 K-H]^{8−}), m/z 1074 ([Q_b + 2 DHII-4CPh + 3 K + NH₄-H]^{8−}), m/z 1257 ([Q_b + K-H]^{6−}), and m/z 1508 ([Q_b + 2NH₄-H]^{5−}). The ions at m/z 696 ([Q_b + 4 K-H]^{11−}), m/z 770 ([Q_b + 5 K-H]^{10−}), m/z 1257 ([Q_b + K-H]^{6−}) and m/z 1508 ([Q_b + 2NH₄-H]^{5−}) correspond to the two hairpin structures formed by d(T₂AG₃)₂ sequence with the charge states of −11, −10, −6, and −5, respectively. The peaks at m/z 977 ([Q_b + DHII-4CPh + 4 K-H]^{16−}), m/z 1001 ([Q_b + DHII-4CPh + K-H]^{8−}), m/z 1017 ([Q_b + DHII-4CPh + 4 K-H]^{8−}) and m/z 1074 ([Q_b + 2DHII-4CPh + 3 K + NH₄-H]^{8−}) can be attributed to the adduct ions formed by the interaction between DHII-4CPh and the d(T₂AG₃)₂ G-quadruplex DNA with the charge states of −16, −8, −8, and −8, respectively. In the ESI-MS experimental data as well as in Table 3, mostly 1:1 stoichiometry between DHII-4CPh and d(T₂AG₃)₂ G-quadruplex was observed. This may be because the experiments were performed at very low derivative and DNA concentration. Even at lower concentration, due to higher and stronger interaction between the DHII-4CPh and the d(T₂AG₃)₂ G-quadruplex molecules, at least one adduct corresponding to 1:2 stoichiometry was noticed (the peak with m/z 1074) in Table 3. However, since ITC titration experiments were carried out at higher concentrations and because of greater affinity and interaction between the DHII-4CPh and the d(T₂AG₃)₂ G-quadruplex DNA molecules, 1:2 stoichiometry was observed. Further, the presence of relatively more number of intense peaks corresponding to DHII-4CPh–d(T₂AG₃)₂ G-quadruplex complex adduct ions in the ESI-MS spectra (Fig. 3D), reflects the existence of more number of DHII-4CPh–G-quadruplex DNA complex molecules in solution. These results

indicate higher interaction of DHII-4CPh with dimeric G-quadruplex formed by d(T₂AG₃)₂ over tetrameric d(T₂AG₃) G-quadruplex.

3.3.2. Binding of DHII-4CPh with two different forms of G-quadruplex at higher concentration using spectroscopy

ESI-MS studies show that DHII-4CPh has higher interaction with dimeric G-quadruplex formed by d(T₂AG₃)₂ than with tetrameric d(T₂AG₃) quadruplex at lower concentration. To reassert the interaction of DHII-4CPh with two different G-quadruplex forms at higher concentrations (μM range), spectroscopy studies were performed. Circular dichroism (CD) spectroscopy has been used to understand the conformational changes in G-quadruplex DNA on interaction with DHII-4CPh. It was reported earlier that parallel G-quadruplexes display a positive band at around 265 nm and a negative band around 240 nm. Similarly, antiparallel G-quadruplexes exhibit a positive band at around 295 nm and negative band around 260 nm [60]. The CD spectrum of 5.0 μM d(T₂AG₃) displays a prominent positive band at 265 nm and a small negative band at 240 nm, suggesting the existence of parallel intermolecular quadruplex in solution [61]. With the addition of 2.5 and 5.0 μM DHII-4CPh, there is a negligible change in the position and the intensity of positive bands (Fig. 4A), indicating a lesser interaction of DHII-4CPh with G-quadruplex formed by d(T₂AG₃). Further, the negative band intensity at 240 nm did not alter much, suggesting no change in the helicity of DNA after DHII-4CPh interaction. These results indicate that DHII-4CPh has less effect on d(T₂AG₃) quadruplex conformation.

On the other hand, the CD spectrum of d(T₂AG₃)₂ G-quadruplex DNA is different. It presents a positive band at 265 nm, a small shoulder at 295 nm and a small negative band at about 240 nm. This suggests the presence of mixed type parallel-antiparallel G-quadruplex DNA [62]. Fig. 4B shows the CD spectrum of 5.0 μM d(T₂AG₃)₂ G-quadruplex DNA before and after the addition of DHII-4CPh. On addition of 2.5 μM and 5.0 μM of DHII-4CPh to d(T₂AG₃)₂ G-quadruplex, the positive bands at 265 nm and 295 nm show considerable hypochromicity without any shift. The hypochromicity of CD band can be ascribed to the partial unfolding of G-quadruplex DNA [63]. Further, the negative band intensity at 240 nm exhibited a gradual decrease, suggesting changes

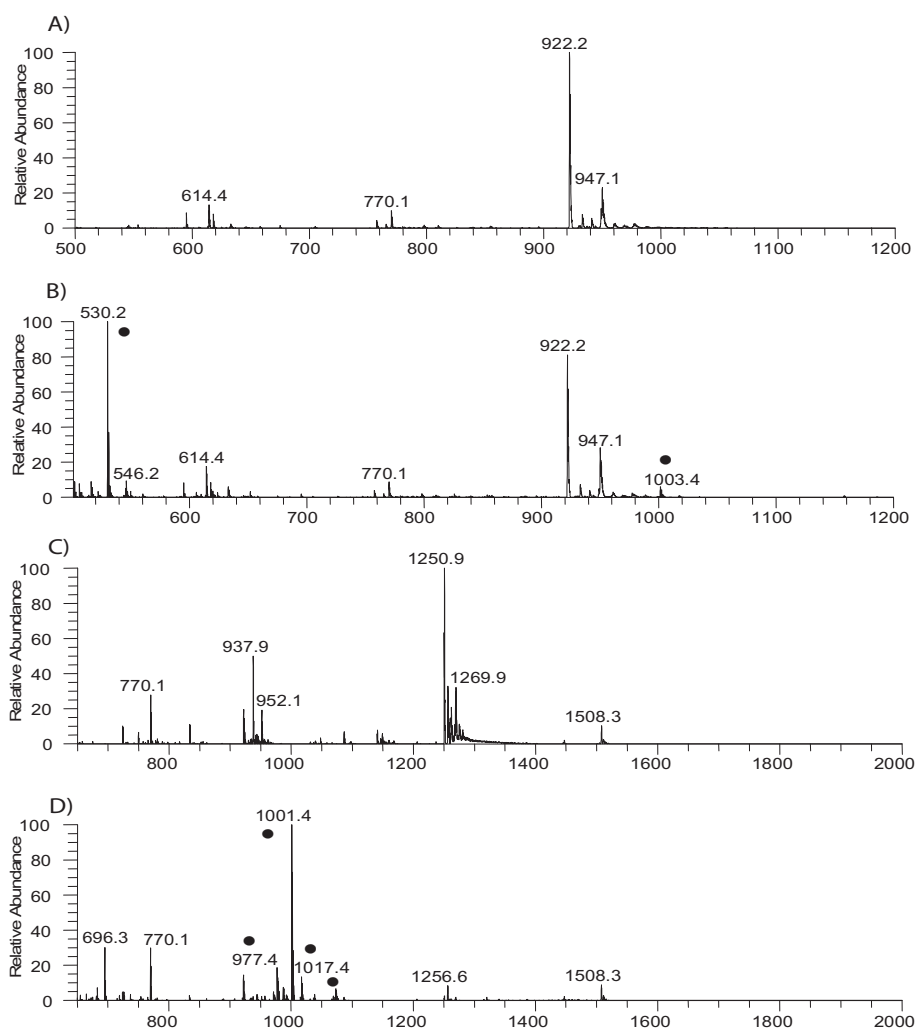


Fig. 3. ESI mass spectra of (A) $d(T_2AG_3)$ G-quadruplex alone, (B) $d(T_2AG_3)$ G-quadruplex with DHII-4CPh, (C) $d(T_2AG_3)_2$ G-quadruplex DNA alone and (D) $d(T_2AG_3)_2$ G-quadruplex with DHII-4CPh. The peaks marked with "*" are adduct ions.

in the DNA helicity. CD experiments emphasize that DHII-4CPh interacts better with G-quadruplex formed by $d(T_2AG_3)_2$ than that formed by $d(T_2AG_3)$ and brings detectable conformational change in the quadruplex formed by $d(T_2AG_3)_2$. These results support the ESI-MS experimental data.

To gain further insight into the interaction between the DHII-4CPh and G-quadruplexes, UV-visible spectra were recorded in the presence and the absence of intermolecular G-quadruplexes formed by $d(T_2AG_3)$ and $d(T_2AG_3)_2$. UV-visible spectrum of DHII-4CPh shows three absorption peaks at 202 nm, 222 nm and 272 nm (Fig. 5A). On addition of

different amounts of $d(T_2AG_3)$ G-quadruplex to DHII-4CPh, the absorption peak exhibited hyperchromicity without any shift. No isobestic point was noticed. By correlating the data with the published results in the literature, indicates that derivative DHII-4CPh binds to the surface of $d(T_2AG_3)$ G-quadruplex DNA [64,65]. UV-visible experiments indicate that, due to the non-covalent surface binding interaction of the DHII-4CPh derivative, less adducts were seen in corresponding ESI-MS spectra. Based on the absorbance values obtained, the DHII-4CPh-DNA binding constant (K_b) was calculated by following the steps mentioned in the experimental procedure. The binding constant obtained with

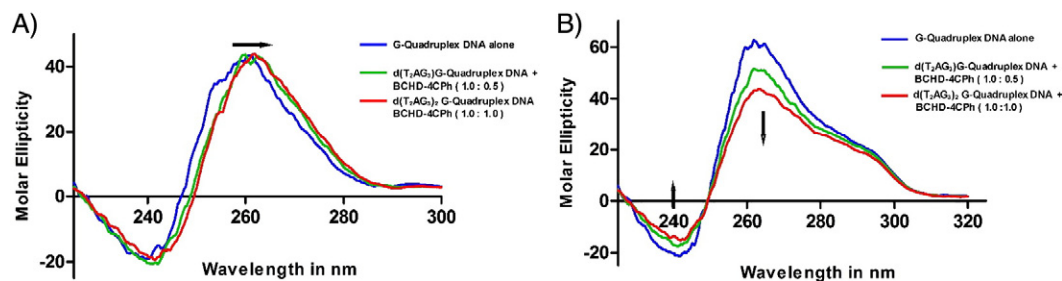


Fig. 4. A & B. CD spectra of $d(T_2AG_3)$ & $d(T_2AG_3)_2$ G-quadruplex in the presence and the absence of DHII-4CPh. To the 5.0 μ M of G-quadruplex DNA in 100 mM KBPS buffer, 2.5 μ M and 5.0 μ M of DHII-4CPh was added. With the addition of DHII-4CPh to $d(T_2AG_3)_2$ G-quadruplex, both the positive and negative band intensities at 265 nm and 240 nm exhibited a gradual reduction. Not much change was noticed when DHII-4CPh was added to $d(T_2AG_3)$ G-quadruplex. The variation in the band intensities was marked with arrows.

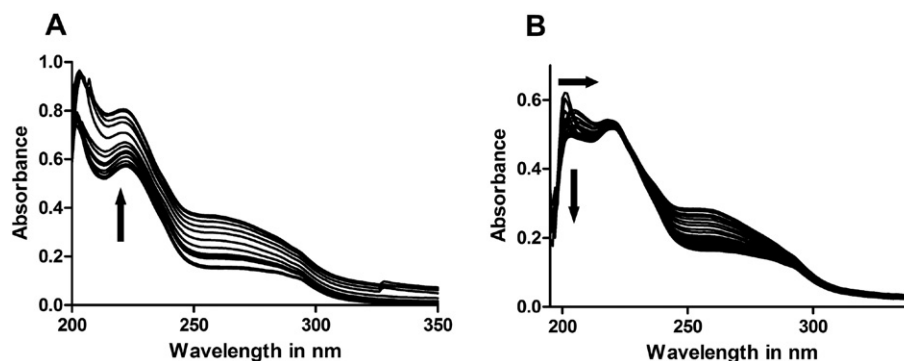


Fig. 5. UV-visible spectrum of (A) DHII-4CPh with d(T₂AG₃) G-quadruplex DNA and (B) DHII-4CPh with d(T₂AG₃)₂ G-quadruplex DNA. 5.0 μ M of DHII-4CPh was prepared in 1:1 methanol: milli Q water and 5.0 μ M of G-quadruplex DNA was prepared in 100 mM KBPS buffer. Each time to 5.0 μ M DHII-4CPh derivative equal aliquots of quadruplex DNA was added.

DHII-4CPh, on interaction with d(T₂AG₃) G-quadruplex DNA was in the 10^3 range ($K_b = 1.8 \times 10^3 \text{ M}^{-1}$).

On the other hand, with the addition of different amounts of d(T₂AG₃)₂ G-quadruplex DNA to DHII-4CPh, the absorption peak at 202 exhibited slight hypochromicity and about 4 nm (202 to 206 nm) bathochromic shift (Fig. 5B). An isobestic point was observed at 230 nm. According to the reported data available in the literature, the hypochromicity accompanied with slight bathochromic shift usually occurs when the derivative intercalate between the two stacks of d(T₂AG₃)₂ G-quadruplex [66]. Hypochromicity of the derivative's absorption peak is due to the interaction between the electronic states of the derivative with quadruplex DNA bases [67] whereas the bathochromic shift is related to the decrease in orbitals after derivative binding to DNA [68]. It was noticed that DHII-4CPh binds to d(T₂AG₃)₂ G-quadruplex DNA with higher affinity which is discernible from its high binding constant, in the 10^5 range ($K_b = 1.1 \times 10^5 \text{ M}^{-1}$). The UV-visible experimental data also make it clear that due to higher interaction and binding of DHII-4CPh to d(T₂AG₃)₂ G-quadruplex DNA, more adducts were observed in the corresponding ESI-MS spectra.

3.4. Effect of G-quadruplex DNA stabilization on in vitro DNA synthesis and gene expression

3.4.1. Levels of c-MYC expression in DHII-4CPh treated cancer cells

Expression of a protein in a cell can be elucidated using quantitative real time PCR. A well-known oncoprotein namely c-MYC expression levels in cancer cells were reported high in cancer cells compared to normal cells [69]. Reduction of oncoprotein levels indicates the ability of a derivative/molecule to induce apoptosis in cancer cells. In order to determine the effect of derivative treatment on c-MYC expression in malignant neoplastic disease cells, B16F10 human melanoma cells (1×10^6) were grown after treating the cells with different concentrations of DHII-4CPh derivative. Interestingly, the expression of c-MYC was found less in B16F10 cells treated with DHII-4CPh, compared to untreated cells. Though the expression of c-MYC was low at 8 μ M DHII-4CPh, the level of expression was reduced to half at around 4 μ M concentration. Endogenous expression levels of β -actin remained the same at all concentrations studied. The gel picture obtained after loading the PCR amplified products on 1.5% agarose gel is shown in Fig. 6A. A graphical representation illustrating band intensities vs concentration of DHII-4CPh (shown in Fig. 6B) indicates that the band intensity reduces to half when the derivative concentration was at around 4 μ M.

RT PCR experiments show that c-MYC expression was reduced in B16F10 cells after DHII-4CPh treatment, indicating its potential to induce apoptosis in cancer cells. Further, the results indicate that it has no consequence on the expression of β -actin when the melanoma cells were treated with a similar concentration of DHII-4CPh.

3.4.2. Suppression of DNA synthesis in vitro by DHII-4CPh through G-quadruplex DNA stabilization

DNA binding experiments show that DHII-4CPh has higher interaction with G-quadruplex DNA and the real time PCR experiments revealed that on DHII-4CPh treatment, the expression of c-MYC has declined without affecting the endogenous expression of housekeeping gene, β -actin. To infer the mechanism of action of DHII-4CPh, when likened to other indolizino indole derivatives, namely DHII-TPh and DHII-MPhPy, in reducing c-MYC expression, stop assay was carried out with the three derivatives at different concentrations. Further, this assay emphasizes the importance of c-MYC G-quadruplex DNA stabilization by indolizino indoles in impeding DNA synthesis and transcription machinery resulting in down-regulation of oncoprotein synthesis in cells.

DNA synthesis products obtained with Pu27 and Pu27 rev primers in the presence of various concentrations of DHII-TPh, DHII-MPhPy and DHII-4CPh are depicted graphically in Fig. 7. The effect of the derivative on in vitro DNA synthesis inhibition, using a non-quadruplex DNA template (Pu27-13, 14), was carried out only with DHII-4CPh, as it has been identified as a potential derivative in previous experiments. The outcome of this assay shows that with 8 μ M DHII-4CPh and Pu27/Pu 27 rev primers the intensity of DNA synthesis bands has brought down to about 10 AU. On the other hand, the DNA band intensity has not altered

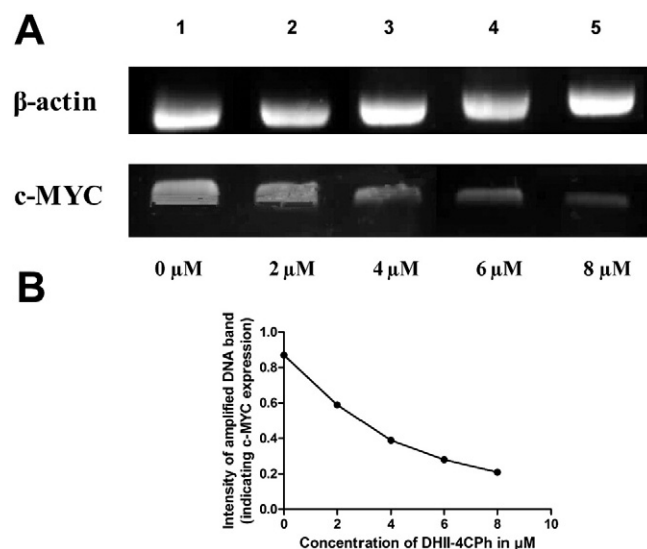


Fig. 6. A. Agarose gel picture showing the PCR amplified products of β -actin and c-MYC after treating the B16F10 cells with different concentrations of DHII-4CPh for 24 h. The concentration of DHII-4CPh in lanes from left to right is 0 μ M, 2 μ M, 4 μ M, 6 μ M, and 8 μ M. B. Graphical representation showing the variation in c-MYC gene expression in B16F10 cells before and after the DHII-4CPh treatment.

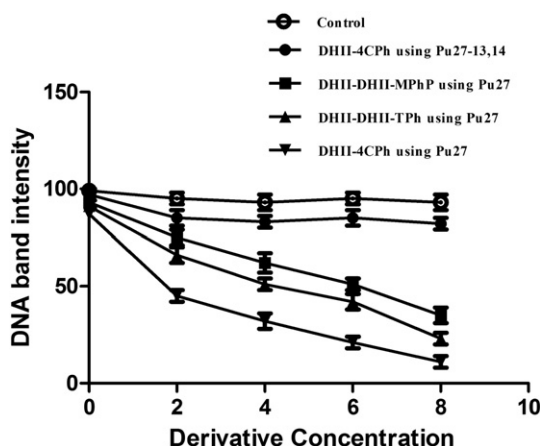


Fig. 7. PCR stop assay. Graphical representation showing the variation in the intensity of DNA bands synthesized in the presence of various concentrations of DHII-4CPh using Pu27-13, 14 as a template (filled circles). Similarly, intensity of DNA bands obtained in the presence of DHII-MPhPy (filled squares), DHII-TPh (filled triangles) and DHII-4CPh (filled inverted triangles) derivative when Pu27 is used as a template. The control samples were represented with open circles.

to a great extent (it rested at roughly 95 AU) when PCR is carried out with Pu27-13, 14 and control. Nevertheless, with DHII-MPhPy and DHII-TPh, the lowest DNA band intensity recorded was ~46 AU and ~25 AU respectively (Fig. 7). Stop assay results reveal that DHII-4CPh inhibited DNA synthesis at the lower concentration range itself (2–4 μM). The gel pictures obtained with each set of sample is shown in Fig. S3. These results support the data obtained from real time PCR experiments. Whereas with DHII-TPh and DHII-MPhPy, DNA synthesis inhibition was noted at higher concentrations ranging 6–8 μM. From the assay results, it is evident that DHII-4CPh stabilizes G-quadruplex DNA and effectively inhibits *in vitro* DNA synthesis. Nevertheless, *in vitro* DNA synthesis was not affected much even in the presence of DHII-4CPh when a non-quadruplex forming DNA (Pu27-13, 14) was used as a template. The outcomes suggest a direct relationship between G-quadruplex DNA stabilization and inhibition of DNA synthesis. Further, higher DNA synthesis inhibition will lead to down-regulation of transcription processes in cells. We hypothesize that in real time PCR experiment, the down-regulation of c-MYC expression upon DHII-4CPh treatment might have taken place due to efficient interaction and stabilization of the G-quadruplex structure formed by the guanine rich sequence of the nuclease hypersensitivity element III1 (NHE III1).

Competitive inhibition by various derivatives and the inhibition constants (K_i) for each of the derivatives was calculated using the Cheng–Prusoff equation (using Eq. (3)). It is $2.82 (\pm 0.067) \mu\text{M}$, $1.81 (\pm 0.058) \mu\text{M}$ and $0.91 (\pm 0.065) \mu\text{M}$ for DHII-MPhPy, DHII-TPh and DHII-4CPh respectively. The observed inhibition constant for DHII-4CPh was low, indicating its ease to interact, stabilize c-MYC G-quadruplex DNA and inhibit *in vitro* DNA synthesis even at lowest substrate concentrations.

3.4.3. Effect of derivatives on endogenous c-MYC gene expression

From real time PCR and stop assay results, it is unmistakable that upon increasing the concentration of DHII-4CPh, reduction in c-MYC expression and enhanced inhibition of DNA synthesis were noticed. To further validate the assay results and to verify the relationship between G-quadruplex DNA stabilization and down-regulation of gene expression, luciferase assay was performed with HeLa cells, transfected with Del 4 and Del 4 mutant plasmids, in the presence and the absence of DHII-4CPh derivative. When HeLa cells with Del 4 plasmid was treated with 2 μM, 4 μM, 6 μM and 8 μM concentrations of DHII-4CPh for 24 h and 48 h, it was strange to observe a significant decrease in relative light units (RLU) from 1.8 ± 0.2 , 1.7 ± 0.3 , 1.5 ± 0.2 , 1.1 ± 0.4 to 1.6 ± 0.1 , 1.5 ± 0.3 , 0.8 ± 0.4 , and 0.5 ± 0.1 respectively. Whereas

the variation in the expression of luciferase was insignificant (from 2.2 ± 0.3 to 2.1 ± 0.2) even after 48 h of treatment, in samples where there is no DHII-4CPh derivative was added (Fig. 8). Variation in luciferase gene expression is apparently due to changes in transcription (rather than translation) because of G-quadruplex DNA stabilization by DHII-4CPh. This was confirmed in the assay with Del 4 mutant plasmids, in which DNA sequence that cannot form G-quadruplex DNA structure was cloned in the place of Del 4 plasmid (details are shown in Fig. S4, under supplementary information). With Del 4 mutant plasmid, after 24 h of incubation with DHII-4CPh (in the same concentration range), there is a negligible change in RLU (from 2.2 ± 0.2 to 2.1 ± 0.1), manifesting same luciferase gene expression irrespective of DHII-4CPh concentration. The results of luciferase assay indicate that the G-quadruplex formation by the c-MYC promoter region sequence and its stabilization by synthetic DHII-4CPh derivative has remarkable effect on c-MYC gene expression. Similar results were reported earlier for the repression of c-MYC and human estrogen receptor alpha through G-quadruplex DNA stabilization [70,71].

3.5. Role of dihydroindolizino indole scaffolds on cancer cell proliferation and anticancer activity

3.5.1. Cell migration assay

It was recognized that reduction in oncoprotein expression would lead to induction of apoptosis and reduction of cancer cell proliferation. The previous biochemical assays indicate that in B16F10 cells treated with DHII-4CPh, the expression of c-MYC (a known oncoprotein) has slimmed down, showing its potential to diminish cancer cell proliferation. To verify the strength of dihydroindolizino indole derivatives as an anti-proliferating agent, human normal and cancer cell lines (CRL-2115, CRL-2120, MCF-7, A549 and B16F10) were grown in the presence and the absence of dihydroindolizino indole derivatives. Among the dihydroindolizino indole scaffolds, 4-cyanophenyl group (DHII-4CPh), demonstrated higher control over the proliferation of tumor cells than normal cells. DHII-4CPh could inhibit cancer cell proliferation at a concentration as low as 3 μM. The outgrowth of cancer cells was relatively high when they were treated with DHII-TPh and DHII-MPhPy. The cells treated with Hermin, a well-known anticancer agent, was considered as a control in this assay. The effect of dihydroindolizino indole derivatives was high in tumor cells compared to normal cells. It may be due to increased metabolism and uptake of derivatives by the rapidly dividing tumor cells over normal cells. Though the exact reasons are not known, this assay indicates that with dihydroindolizino indole derivatives, the percentage of viable cells are less when they are given to B16F10 cells, indicating their higher potential in melanoma cell lines

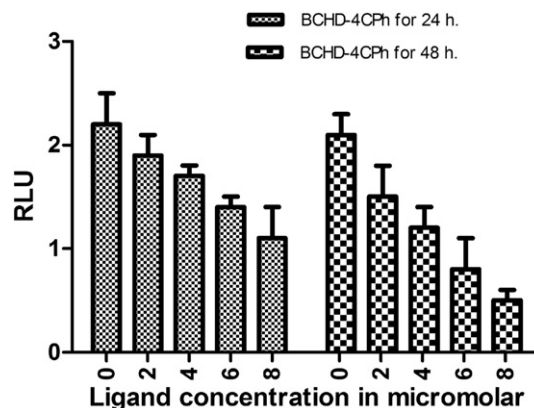


Fig. 8. Bar chart showing the reduction in the reporter activity after 24 h and 48 h of derivative treated HeLa cells transfected with Del 4 plasmid (which consists of quadruplex forming c-MYC sequence) in the comportment of a DHII-4CPh derivative. The error bars indicate stranded errors over three independent experiments.

Table 4

Cell migration assay results obtained when dihydroindolizino indole derivatives (DHII) were incubated with normal and tumor cells for 24 h.

S.No.	Derivative name	Maximum cell proliferation inhibition (concentration in μM)				
		CRL-2115	CRL-2120	MCF-7	B16F10	A549
1.	Hermine	38.8 \pm 0.4	36.7 \pm 0.6	17.6 \pm 0.8	6.2 \pm 0.6	14.3 \pm 0.9
2.	DHII-4CPh	16.4 \pm 0.6	16.7 \pm 0.5	9.2 \pm 0.9	3.7 \pm 0.4	6.5 \pm 0.8
3.	DHII-TPh	15.9 \pm 0.6	15.4 \pm 0.8	11.2 \pm 0.7	8.1 \pm 0.4	12.9 \pm 0.6
4.	DHII-MPhPy	16.1 \pm 0.4	16.6 \pm 0.7	12.8 \pm 0.4	9.4 \pm 0.5	13.1 \pm 0.7

than in any other tumor cell lines. The data obtained from this assay is shown in Table 4.

4. Conclusions

In the present study, three different dihydroindolizino indole derivatives were synthesized and studied for their ability to selectively stabilize G-quadruplex DNA and inhibit the proliferation of malignant neoplastic disease cells. Among the derivatives, DHII-4CPh has a higher interaction with G-quadruplex DNA and selectively stabilizes G-quadruplex DNA over dsDNA. Among intermolecular quadruplexes, interaction of DHII-4CPh is higher with dimeric G-quadruplex formed by $d(\text{T}_2\text{AG}_3)_2$ than with tetrameric structure formed by $d(\text{T}_2\text{AG}_3)_4$. Spectroscopy results support the ESI-MS data and confirms that DHII-4CPh exhibit higher affinity and stronger interaction with $d(\text{T}_2\text{AG}_3)_2$ quadruplex DNA. DHII-4CPh derivative down-regulates c-MYC expression in tumor cells. In vitro DNA synthesis using the template and primers from the nuclease hypersensitivity element III1 (NHE III1) region and luciferase reporter assay indicates that c-MYC promoter transcription is gradually down regulated with an increase of the DHII-4CPh concentration, in all likelihood due to G-quadruplex DNA stabilization. Cell migration assay confirms that the dihydroindolizino indole derivatives will significantly reduce proliferation of the cancer cells in the micro molar concentration range. Among the dihydroindolizino indole derivatives, DHII-4CPh exhibited the highest and selective affinity, interaction and stability toward G-quadruplex DNA, reduced c-MYC expression, brings down cancer cell proliferation and induced apoptosis among cancer cells. Such studies will be useful to identify and develop suitable lead derivatives, which have specific interaction with G-quadruplex DNA and exhibit potential anticancer activity.

Abbreviations

DHII-4CPh methyl-3-benzyl-11-(4-cyanophenyl)-6-methyl-6,11-dihydro-5H-indolizino [6,7-b] indole-1-carboxylate.
 DHII-TPh methyl-3-benzyl-6-methyl-11-(thiophen-2-yl)-6,11-dihydro-5H-indolizino [6,7-b] indole-1-carboxylate.
 DHII-MPhPy methyl-3-benzyl-6-methyl-11-(3-methyl-1-phenyl-1H-pyrazol-4-yl)-6,11-dihydro-5H-indolizino[6,7-b]indole-1-carboxylate.
 PTSA p-toluenesulfonic acid.

Acknowledgment

The authors thank the Director, CSIR-CCMB and CSIR-IICT, Hyderabad for their encouragement and support. G. R., P. R. and M. D. R. thank UGC and CSIR, respectively for the Research Fellowship. N. N. is thankful to Indo Swiss Joint Research Programme (ISJRP) for the partial financial support (Grant number CH: 138844) and Dr. T. Ramakrishna and Dr. Vijaya Gopal for carefully going through the manuscript. We thank Prof. Bert Vogelstein for providing Del 4, which was originally gifted to Dr. Shantanu Chowdhury. We also thank Dr. Shantanu Chowdhury for gifting the Del 4 mutant plasmid.

Appendix A. Supplementary data

Supplementary data to this article can be found online at <http://dx.doi.org/10.1016/j.bbagen.2014.10.004>.

References

- [1] L.C. Tu, C.S. Chen, I.C. Hsiao, J.W. Chern, C.H. Lin, Y.C. Shen, S.F. Yeh, The beta-carboline analog Mana-Hox causes mitotic aberration by interacting with DNA, *Chem. Biol.* 12 (2005) 1317–1324.
- [2] Z. Chen, R. Cao, B. Shi, L. Guo, J. Sun, Q. Ma, W. Fan, H. Song, Synthesis and biological evaluation of 1,9-disubstituted β -carbolines as potent DNA intercalating and cytotoxic agents, *Eur. J. Med. Chem.* 46 (2011) 5127–5137.
- [3] T. Golob, R. Liebl, E. Von Angerer, Sulfamoyloxy-substituted 2-phenylindoles: antiestrogen based inhibitors of the steroid sulfatase in human breast cancer cells, *Bioorg. Med. Chem.* 10 (2002) 3941–3953.
- [4] C.H. Nguyen, J.M. Lhoste, F. Lavelle, M.C. Bissery, E. Bisagni, Synthesis and antitumor activity of 1-[(dialkylamino) alkyl]amino-4-methyl-5Hpyrido[4,3-b]-(benzo[e]- and benzo [g]) indoles. A new class of antineoplastic agents, *J. Med. Chem.* 33 (1990) 1519–1528.
- [5] O. Güzel, N. Karali, A. Salman, Synthesis and antituberculosis activity of 5-methyl/trifluoro-methoxy-1H-indole-2,3-dione 3-thiosemicarbazone derivatives, *Bioorg. Med. Chem.* 16 (2008) 8976–8987.
- [6] P. Thirumurugan, S. Mahalakshmi, P.T. Perumal, Synthesis and anti-inflammatory activity of 3-indolyl pyridine derivatives through one-pot multi component reaction, *J. Chem. Sci.* 122 (2010) 819–832.
- [7] S. Hayashi, Y. Sumi, N. Ueno, A. Murase, J. Takada, Discovery of a novel COX-2 inhibitor as an orally potent anti-pyretic and antiinflammatory drug: design, synthesis and structure-activity relationship, *Biochem. Pharmacol.* 82 (2011) 755–768.
- [8] A.S. Guerra, D.J. Malta, L.P. Laranjeira, M.B. Maia, N.C. Colaço, C. De Lima Mdo, S.L. Galdino, R. Pitta Ida, T. Gonçalves-Silva, Anti-inflammatory and anti-nociceptive activities of indole-imidazolidine derivatives, *Int. Immunopharmacol.* 11 (2011) 1816–1822.
- [9] T. Luker, R. Bonnert, S. Brough, A.R. Cook, M.R. Dickinson, I. Dougall, C. Logan, Substituted indole-1-acetic acids as potent and selective CRTh2 antagonists-discovery of AZD1981, *Bioorg. Med. Chem. Lett.* 21 (2011) 6288–6292.
- [10] (a) W.K. Anderson, H.L. McPherson, J.S. New, A.C. Rick, Synthesis and murine antineoplastic activity of bis[(carbamoyloxy)methyl] derivatives of pyrrolo [2,1-a]isoquinoline, *J. Med. Chem.* 27 (1984) 1321–1325;
 (b) R. Chaniyara, N. Kapuriya, H. Dong, P.C. Lee, S. Suman, B. Marvania, T.C. Chou, T.C. Lee, R. Kakadiya, A. Shah, T.L. Su, Novel bi-functional alkylating agents, 5,10-dihydropyrrolo[1,2-b]isoquinoline derivatives, synthesis and biological activity, *Bioorg. Med. Chem.* 19 (1) (2011) 275–286.
- [11] R. Chaniyara, S. Tala, C.-W. Chen, X. Zang, R. Kakadiya, L.-F. Lin, C.-H. Chen, S.-I. Chien, T.-C. Chou, T.-H. Tsai, T.-C. Lee, A. Shah, T.-L. Su, Novel antitumor indolizino [6,7-b]indoles with multiple modes of action: DNA cross-linking and topoisomerase I and II inhibition, *J. Med. Chem.* 56 (2013) 1544–1563.
- [12] L.H. Hurley, D.D. Von Hoff, A. Siddiqui-Jain, D. Yang, Drug targeting of the c-MYC Promoter to repress gene expression via a G-quadruplex silencer element, *Semin. Oncol.* 33 (4) (2006) 498–512.
- [13] A. Siddiqui-Jain, C.L. Grand, D.J. Bearss, L.H. Hurley, Direct evidence for a G-quadruplex in a promoter region and its targeting with a small molecule to repress c-MYC transcription, *Proc. Natl. Acad. Sci. U. S. A.* 99 (18) (2002) 11593–11598.
- [14] A. DeCian, L. Lacroix, C. Douarre, N. Temime-Smaali, C. Trentesaux, J.-F. Riou, J.-L. Mergny, Targeting telomeres and telomerase, *Biochimie* 90 (1) (2008) 131–155.
- [15] S. Neidle, G. Parkinson, Telomere maintenance as a target for anticancer drug discovery, *Nat. Rev. Drug Discov.* 1 (5) (2002) 383–393.
- [16] L. Oganessian, T.M. Bryan, Physiological relevance of telomeric G-quadruplex formation: a potential drug target, *BioEssays* 29 (2) (2007) 155–165.
- [17] H.M. Lee, D.S. Chan, F. Yang, H.Y. Lam, S.C. Yan, C.M. Che, D.L. Ma, C.H. Leung, Identification of natural product fonsicin B as a stabilizing ligand of c-myc G-quadruplex DNA by high-throughput virtual screening, *Chem. Commun.* 46 (2010) 4680–4682.
- [18] D.S. Chan, H. Yang, M.H. Kwan, Z. Cheng, P. Lee, L.P. Bai, Z.H. Jiang, C.Y. Wong, W.F. Fong, C.H. Leung, D.L. Ma, Structure-based optimization of FDA-approved drug methylene blue as a c-myc G-quadruplex DNA stabilizer, *Biochimie* 93 (2011) 1055–1064.
- [19] D.L. Ma, D.S. Chan, W.C. Fu, H.Z. He, H. Yang, S.C. Yan, C.H. Leung, Discovery of a natural product-like c-myc G-quadruplex DNA groove-binder by molecular docking, *PLoS One* 7 (2012) e43278.
- [20] H. Yang, H.J. Zhong, K.H. Leung, D.S.H. Chan, V.P.Y. Ma, W.C. Fu, R. Nanjunda, W.D. Wilson, D.L. Ma, C.H. Leung, Structure-based design of flavone derivatives as c-myc oncogene down-regulators, *Eur. J. Pharm. Sci.* 48 (2013) 130–141.
- [21] H. Yang, V.P.Y. Ma, D.S.H. Chan, C.H. Leung, D.L. Ma, A cyclometallated iridium(III) complex as a c-myc G-quadruplex stabilizer and down-regulator of c-myc oncogene expression, *Curr. Med. Chem.* 20 (2013) 576–582.
- [22] N. Nagesh, V.K. Sharma, A. Ganesh Kumar, E.A. Lewis, Effect of ionic strength on porphyrin drugs interaction with quadruplex DNA formed by the promoter region of C-myc and Bcl2 oncogenes, *J. Nucleic Acids* (2010), <http://dx.doi.org/10.4061/2010/146418>.
- [23] N. Nagesh, R. Buscaglia, J.M. Dettler, E.A. Lewis, Studies on the site and mode of TMPyP4 interactions with Bcl-2 promoter sequence G-quadruplexes, *Biophys. J.* 98 (1) (2010) 2628–2633.
- [24] N. Nagesh, A. Krishnaiah, A comparative study on the interaction of acridine and synthetic bis-acridine with G-quadruplex structure, *J. Biochem. Biophys. Methods* 57 (1) (2003) 65–74.

- [25] F. Koepfel, J.F. Riou, A. Laoui, P. Mailliet, P.B. Arimondo, Ethidium derivatives bind to G-quartets, inhibit telomerase and act as fluorescent probes for quadruplexes, *Nucleic Acids Res.* 29 (5) (2001) 1087–1096.
- [26] G.R. Clark, P.D. Pytel, C.J. Squire, S. Neidle, Structure of the first parallel DNA quadruplex–drug complex, *J. Am. Chem. Soc.* 125 (14) (2003) 4066–4067.
- [27] W. Tuntiwachapikul, J.T. Lee, M. Salazar, Design and synthesis of the G-quadruplex – specific cleaving reagent perylene-EDTA.iron(II), *J. Am. Chem. Soc.* 123 (2001) 5606–5607.
- [28] M.Y. Kim, H. Vankayalapati, K. Shin-ya, K. Wierzbicka, L.H. Hurley, Telomestatin, a potent telomerase inhibitor that interacts quite specifically with the human telomeric intra-molecular G-quadruplex, *J. Am. Chem. Soc.* 124 (10) (2002) 2098–2099.
- [29] N. Nagesh, D. Chatterji, Ammonium ion at low concentration stabilizes the G-quadruplex formation by telomeric sequence, *J. Biochem. Biophys. Methods* 30 (1) (1995) 1–8.
- [30] N. Nagesh, A. Krishnaiah, V.M. Dhople, C.S. Sundaram, M.V. Jagannadham, Noncovalent interaction of G-quadruplex DNA with acridine at low concentration monitored by MALDI-TOF mass spectrometry, *Nucleosides Nucleotides Nucleic Acids* 26 (3) (2007) 303–315.
- [31] Y. Qin, L.H. Hurley, Structures, folding patterns, and functions of intramolecular DNA G-quadruplexes found in eukaryotic promoter regions, *Biochimie* 90 (2008) 1149–1171.
- [32] D.J. Patel, A.T. Phan, V. Kuryavyi, Human telomere, oncogenic promoter and 5'-UTR G-quadruplexes: diverse higher order DNA and RNA targets for cancer therapeutics, *Nucleic Acids Res.* 35 (2007) 7429–7455.
- [33] A. Rangan, O.Y. Fedoroff, L.H. Hurley, Induction of duplex to G-Quadruplex transition in the c-myc promoter region by a small molecule, *J. Biol. Chem.* 276 (7) (2001) 4640–4646.
- [34] A.K. Todd, S.M. Haider, G.N. Parkinson, S. Neidle, Sequence occurrence and structural uniqueness of a G-quadruplex in the human c-kit promoter, *Nucleic Acids Res.* 35 (2007) 5799–5808.
- [35] E.M. Rezler, D.J. Bearss, L.H. Hurley, Telomere inhibition and telomere disruption as processes for drug targeting, *Annu. Rev. Pharmacol. Toxicol.* 43 (2003) 359–379.
- [36] M. Fry, L.A. Loeb, The fragile X syndrome d(CGG)_n nucleotide repeats form a stable tetrahelical structure, *Proc. Natl. Acad. Sci. U. S. A.* 91 (11) (1994) 4950–4954.
- [37] G. Biffi, D. Tannahill, J. McCafferty, S. Balasubramanian, Quantitative visualization of DNA G-quadruplex structures in human cells, *Nat. Chem.* 5 (3) (2013) 182–186.
- [38] J.L. Mergny, J.F. Riou, P. Mailliet, M.P. Teulade-Fichou, E. Gilson, Natural and pharmacological regulation of telomerase, *Nucleic Acids Res.* 30 (2002) 839–865.
- [39] J.T. Davis, G-quartets 40 years later: from 5'-GMP to molecular biology and supramolecular chemistry, *Angew. Chem. Int. Ed. Engl.* 43 (6) (2004) 668–698.
- [40] S. Burge, G.N. Parkinson, P. Hazel, A.K. Todd, S. Neidle, Quadruplex DNA: sequence, topology and structure, *Nucleic Acids Res.* 34 (19) (2006) 5402–5415.
- [41] A. Kamal, V. Srinivasulu, V. Lakshma Nayak, M. Satish, N. Shankaraiah, C. Bagul, N.V. Subba Reddy, N. Rangaraj, N. Nagesh, Design and Synthesis of C3-Pyrazole / Chalcone-Linked Beta-Carboline Hybrids: Antitopoisomerase I, DNA-Interactive, and Apoptosis-Inducing Anticancer Agents, *Chemmedchem* (2014), <http://dx.doi.org/10.1002/cmde.201300406>.
- [42] A. Ambrus, D. Chen, J. Dai, T. Bialis, R.J. Jones, D. Yang, Human telomeric sequence forms a hybrid-type intramolecular G-quadruplex structure with mixed parallel/antiparallel strands in potassium solution, *Nucleic Acids Res.* 34 (9) (2006) 2723–2735.
- [43] K. Paeschke, T. Simonsson, J. Postberg, D. Rhodes, H.J. Lipps, Telomere end-binding proteins control the formation of G-quadruplex DNA structures *in vivo*, *Nat. Struct. Mol. Biol.* 12 (10) (2005) 847–854.
- [44] R.I. Mathad, E. Hatzakis, J. Dai, D. Yang, c-MYC promoter G-quadruplex formed at the 5'-end of NHE III1 element: insights into biological relevance and parallel-stranded G-quadruplex stability, *Nucleic Acids Res.* 39 (20) (2011) 9023–9033.
- [45] A. Brown, Analysis of cooperativity by isothermal titration calorimetry, *Int. J. Mol. Sci.* 10 (2009) 3457–3477.
- [46] T.-M. Ou, Y.-J. Lu, C. Zhang, Z.-S. Huang, X.-D. Wang, J.-H. Tan, Y. Chen, D.-L. Ma, K.-Y. Wong, J.C.-O. Tang, A.S.-C. Gu, L.-Q. Chan, Stabilization of G-quadruplex DNA and down-regulation of oncogene c-myc by quindoline derivatives, *J. Med. Chem.* 50 (2007) 1465–1474.
- [47] R.K. Thakur, P. Kumar, K. Halder, A. Verma, A. Kar, J.L. Parent, R. Basundra, A. Kumar, S. Chowdhury, Metastases suppressor NM23-H2 interaction with G-quadruplex DNA within c-MYC promoter nuclease hypersensitive element induces c-MYC expression, *Nucleic Acids Res.* 37 (2009) 172–183.
- [48] P. Chomczynski, N. Sacchi, The single-step method of RNA isolation by acid guanidinium thiocyanate-phenol-chloroform extraction: twenty-something years on, *Nat. Protoc.* 1 (2006) 581–585.
- [49] L. Xu, X. Deng, Protein kinase C α promotes nicotine-induced migration and invasion of cancer cells via phosphorylation of micro- and m-calpains, *J. Biol. Chem.* 281 (2006) 4457–4466.
- [50] C.R. Reddy, M. Damoder Reddy, B. Srikanth, Phosphine-mediated cascade reaction of azides with MBH-acetates of acetylenic aldehydes to substituted pyrroles: a facile access to N-fused pyrrolo-heterocycles, *Org. Biomol. Chem.* 10 (21) (2012) 4280–4288.
- [51] C.V. Kumar, E.H. Asuncion, DNA binding studies and site selective fluorescence sensitization of an anthryl probe, *J. Am. Chem. Soc.* 115 (19) (1993) 8547–8553.
- [52] J.B. Chaires, Inhibition of the thermally driven B to Z transition by intercalating drugs, *Biochemistry* 25 (26) (1986) 8436–8439.
- [53] J.E. Ladbury, B.Z. Chowdhry, Sensing the heat: the application of isothermal titration calorimetry to thermodynamic studies of biomolecular interactions, *Chem. Biol.* 3 (1996) 791–801.
- [54] P. Rahul, P.J. Hergenrother, DNA as a target for anticancer compounds: methods to determine the mode of binding and the mechanism of action, *Curr. Opin. Biotechnol.* 19 (2007) 497–503.
- [55] S.A. Hofstadler, K.A. Sannes-Lowery, Applications of ESI-MS in drug discovery: interrogation of noncovalent complexes, *Nat. Rev.* 5 (7) (2006) 585–595.
- [56] G. Yuan, Q. Zhang, J. Zhou, H. Li, Mass spectrometry of G-quadruplex DNA: formation, recognition, property, conversion, and conformation, *Mass Spectrom. Rev.* 30 (6) (2011) 1121–1142.
- [57] F. Rosu, V. Gabelica, H. Poncelet, E. De Pauw, Tetramolecular G-quadruplex formation pathways studied by electrospray mass spectrometry, *Nucleic Acids Res.* 38 (15) (2010) 5217–5225.
- [58] B. Qiu, Z. Qin, J. Liu, H. Luo, Thymine quintets and their higher order assemblies studied by electrospray ionization mass spectrometry and theoretical calculation, *J. Mass Spectrom.* 46 (6) (2011) 587–594.
- [59] F. Rosu, V. Gabelica, C. Houssier, P. Colson, E.T. De Pauw, Triplex and quadruplex DNA structures studied by electrospray mass spectrometry, *Rapid Commun. Mass Spectrom.* 16 (18) (2002) 1729–1736.
- [60] I.N. Rujan, J.C. Meleney, P.H. Bolton, Vertebrate telomere repeat DNAs favor external loop propeller quadruplex structures in the presence of high concentrations of potassium, *Nucleic Acids Res.* 33 (6) (2005) 2022–2031.
- [61] S. Paramasivan, I. Rujan, P.H. Bolton, Circular dichroism of quadruplex DNAs: applications to structure, cation effects and derivative binding, *Methods* 43 (2007) 324–331.
- [62] W. Li, P. Wu, T. Ohmichi, N. Sugimoto, Characterization and thermodynamic properties of quadruplex/duplex competition, *FEBS Lett.* 526 (2002) 77–81.
- [63] H. Fukuda, M. Katahira, N. Tsuchiya, Y. Enokizono, T. Sugimura, M. Nagao, H. Nakagama, Unfolding of quadruplex structure in the G-rich strand of the minisatellite repeat by the binding protein UP1, *Proc. Natl. Acad. Sci. U. S. A.* 99 (20) (2002) 12685–12690.
- [64] R.F. Pasternack, E.J. Gibbs, J.J. Villafranca, Interactions of porphyrins with nucleic acids, *Biochemistry* 22 (10) (1983) 2406–2414.
- [65] C. Prati, J. Bernadou, B. Meunier, DNA and RNA cleavage by metal complexes, *Adv. Inorg. Chem.* 45 (1998) 251–312.
- [66] O. Hisatsugu, I. Hiroyasu, U. Yoshio, Intercalation of water-soluble bis-porphyrins into poly(dA)–poly(dT) double helix, *Bioorg. Med. Chem.* 9 (12) (2001) 3301–3307.
- [67] B.D. Wang, Z.Y. Yang, P. Crewdson, D.Q. Wang, Synthesis, crystal structure and DNA-binding studies of the Ln(III) complex with 6-hydroxychromone-3-carbaldehyde benzoyl hydrazone, *J. Inorg. Biochem.* 101 (10) (2007) 1492–1504.
- [68] F. Arjmand, M. Aziz, Synthesis and characterization of dinuclear macrocyclic cobalt(II), copper(II) and zinc(II) complexes derived from 2,2,2',2'-S, S[bis(bis-N, N-2-Thiobenzimidazole)oxy]oxalato-1,2-ethane]]: DNA binding and cleavage studies, *Eur. J. Med. Chem.* 44 (2) (2009) 834–844.
- [69] C.Y. Lin, J. Loven, P.B. Rahl, R.M. Paranal, C.B. Burge, J.E. Bradner, T.I. Lee, R.A. Young, Transcriptional amplification in tumor cells with elevated c-MYC, *Cell* 151 (2012) 56–67.
- [70] R.K. Thakur, P. Kumar, K. Halder, A. Verma, A. Kar, J.L. Parent, R. Basundra, A. Kumar, S. Chowdhury, Metastases suppressor NM23-H2 interaction with G-quadruplex DNA within c-MYC promoter nuclease hypersensitive element induces c-MYC expression, *Nucleic Acids Res.* 37 (2008) 172–183.
- [71] G.D. Balkwill, K. Derecka, T.P. Garner, C. Hodgman, A.P. Flint, M.S. Searle, Repression of translation of human estrogen receptor alpha by G-quadruplex formation, *Biochemistry* 48 (2009) 11487–11495.